

Transition radiation by matter-wave solitons in optical lattices

A.V. Yulin, D.V. Skryabin, and P.St.J. Russell

Department of Physics, University of Bath, Bath BA2 7AY, United Kingdom

We demonstrate that matter-wave solitary pulses formed from Bose condensed atoms moving inside optical lattices continuously radiate dispersive matter waves with prescribed momentum. Our analytical results for the radiation parameters and the soliton decay rate are found to be in excellent agreement with numerical modelling performed for experimentally relevant parameters.

Recent observations of matter-wave solitons [1,2] have clearly been amongst the most breaking achievements in the burgeoning field of Bose-Einstein condensation of dilute atomic gases. Balance between the spatial dispersion of matter waves and repulsive or attractive interatomic interactions ensures existence of dark [1] or bright [2] solitons, respectively. Dispersion of the atomic condensates can, however, be reversed by embedding the condensate into a periodic potential created by standing light waves, i.e. *optical lattice* [3–5]. The idea of changing the dispersion sign and of the possible observation of the bright matter-wave solitons in the condensates with repulsive interatomic interaction has been around for a while, see [7] and references therein, and more theoretical results have been produced recently, see, e.g., [8–10], in the view of the rapid maturing of the experimental techniques [3–5]. The concept of the dispersion control by periodic potentials is also well known in solid-state physics [11] and a very active topic of research in nonlinear optics, see, e.g., [12].

To understand the initial motivation which leads to the results described below, it is instructive to recall the effect of the *transition radiation* known from classical electrodynamics [13]. Transition radiation is a continuous emission of electromagnetic waves by a charged particle moving with a *constant* velocity in spatially inhomogeneous medium. This radiation is emitted because the field created by the particle has different characteristics in different parts of the medium. When the particle moves, the field reorganizes itself continuously and shakes off some of its parts in form of the radiation. We expect that similar phenomenon should take place with matter-wave solitons in optical lattices.

In order to change the dispersion sign of matter waves forming the initially resting one-dimensional packet embedded into the optical lattice, one needs to position it in momentum space somewhere between the inflection point of the energy-momentum, i.e., dispersion, characteristic and the edge of the Brillouin zone, see Fig. 1(a) [14]. Only exactly at the edge of the zone does the group velocity go to zero. Solitons with a spread of quasi-momenta centered at the edge will therefore be the only resting bright solitons in the condensates with repulsive inter-atomic interaction. Our primary interest below is, however, moving solitons. Once a solitonic wave packet moves through the periodic potential one can expect that

its structure will not be able to instantly readjust itself to perfectly fit the conditions that the local density maxima are positioned at the center of the local potential minima. Therefore the moving soliton has to continuously overcome the energy barrier, which leads to the continuous emission of matter waves. This energy barrier is analogous to the Peierls-Nabarro potential known for the solitons in discrete systems [6]. Using analogy with the electromagnetic case we term this effect as transition radiation of matter waves.

We start our analysis from the Gross-Pitaevskii (GP) equation describing evolution of the macroscopic wave function of the zero-temperature Bose-Einstein condensate (BEC) interacting with off-resonant standing light wave. We assume that the condensate is tightly confined by the external harmonic potential along the Y and Z directions having the trap frequencies $\omega_{Y,Z} = 2\pi \times 400\text{s}^{-1}$ and that any deviations of the potential along X -axis from the $\sin^2 k_l X$ produced by the intensity of the standing laser field with wavenumber k_l can be disregarded. We take for our estimates that $k_l = 2\pi/800\text{nm}^{-1}$ and consider BEC made of ^{87}Rb atoms with a two-body scattering length $a \simeq 5.4 \times 10^{-9}\text{m}$. The characteristic transverse width of this BEC is then given by $w = \sqrt{\hbar/(m\omega_Y)} \simeq 0.5\mu\text{m}$. Assuming that the condensate profile along the Y, Z directions is given by the lowest mode of the harmonic potential, we can derive the one-dimensional GP equation, which describes dynamics of the X dependent part of the full wave function. The dimensionless normalized form of this equation is [9]:

$$i\partial_t \psi = -\partial_x^2 \psi - \beta \psi \cos 2x + |\psi|^2 \psi. \quad (1)$$

Here the dimensionless time t and spatial coordinate x are measured respectively in the units of $T_0 = 2m/(\hbar k_l^2) \simeq 5 \times 10^{-5}\text{s}$ and $1/k_l \simeq 0.13\mu\text{m}$. Meaning of the dimensionless parameter β is easily inferred from the expression for the lattice potential in the physical units, which is taken as $4\beta E_r \sin^2 k_l X$, where $E_r = \hbar^2 k_l^2/(2m) \simeq \hbar \times 20\text{kHz}$ is the recoil energy. To estimate number of atoms N in the condensate we introduce the effective area in the (Y, Z) -plane, $A_{\text{eff}} = 2\pi w^2 \simeq 1.5\mu\text{m}^2$, and the atom density $n \simeq 10^{14}\text{cm}^{-3}$. Then $N = \int |\psi|^2 dx \times A_{\text{eff}}^2 k_l n^{2/3} / (8\pi|a|) \simeq 4 \times 10^3 \times \int |\psi|^2 dx$.

We proceed by expanding ψ over the Bloch functions, $b(x, k)$ [11]: $\psi(x, t) = \int dk \tilde{\psi}(k, t) b(x, k)$. Here $b(x, k)$ are eigenfunctions of the operator $\hat{L} = \partial_x^2 + \beta \cos 2x$, such

that $\hat{L}b = -\epsilon(k)b$, where k is the quasi-momentum introduced as $b(x, k) = g(x, k)e^{ikx}$ [11], $\epsilon(k)$ is the energy of the non-interacting, i.e. linear, matter-waves, and $g(x, k)$ is the function with the spatial period π . The first allowed, first forbidden (gap) and a small part of the 2nd allowed energy bands are shown in the energy-momentum plot in Fig. 1(a).

Choosing $k = k_s \in [-1, 1]$, we expand $g(x, k)$ in a Taylor series around $k = k_s$ and demonstrate that

$$\psi(x, t) = e^{ik_s x} \hat{G}_s A(x, t). \quad (2)$$

Here, $A(x, t) = \int dk \tilde{\psi}(k, t) e^{i(k-k_s)x}$ and \hat{G}_s is the linear differential operator: $\hat{G}_s = \sum_{n=0}^{\infty} (1/n!) \partial_k^n g(x, k_s) (-i\partial_x)^n$. Similarly $\hat{L}\psi$ can be represented as

$$\hat{L}\psi = -e^{ik_s x} \hat{G}_s \hat{\mathcal{E}}_s [-i\partial_x] A(x, t), \quad (3)$$

where $\hat{\mathcal{E}}_s [-i\partial_x] = \sum_{m=0}^{\infty} (1/m!) \partial_k^m \epsilon(k_s) (-i\partial_x)^m$ is the energy operator. Subscript 's' refers to quantities and functions calculated for $k = k_s$.

After substitution of Eqs. (2), (3) into Eq. (1), we then replace \hat{G}_s with its 1st order approximation $g(x, k_s) \equiv g_s$ and $\hat{\mathcal{E}}_s$ with $\hat{\mathcal{E}}_{2s} \equiv \epsilon_s - i\epsilon'_s \partial_x - 1/2\epsilon''_s \partial_x^2$. Here ϵ'_s and ϵ''_s are, respectively, group velocity and group velocity dispersion of matter-waves. Assuming smallness of the nonlinearity and averaging the resulting equation over g_s we derive the renowned nonlinear Schrödinger (NLS) equation $i\partial_t A = \hat{\mathcal{E}}_{2s} A + \alpha_s |A|^2 A$, where $\alpha_s = \int dx |g_s|^4$. Below we are interested in the bright solitons with ϵ_s belonging to the first allowed energy band. These are given by $A_s = R_s(\xi) \exp\{-ik\tau - i\epsilon_s t\}$, where

$$R_s(\xi) = \sqrt{\frac{2\kappa}{\alpha_s}} \operatorname{sech} \left\{ \xi \sqrt{\frac{2\kappa}{-\epsilon''_s}} \right\}, \quad \xi = x - \epsilon'_s t, \quad (4)$$

$sgn\kappa = sgn\alpha_s = -sgn\epsilon''_s$ and $\kappa \neq 0$ is the nonlinearity induced energy shift. Details of the derivation of NLS equation from Eq. (1) has been previously published using the method of multiple scales [15]. Approximations made above and in [15] imply that ψ has sufficiently narrow spread of quasi-momenta around $k = k_s$. However, the approach introduced here is readily adaptable to give an access to the small amplitude corrections having quasi-momenta detuned far from k_s , see Eqs. (8), (9) below. Note, here that mobile envelope solitons (4) are very different in their properties from practically immobile solitons occupying primarily one or few lattice sites and considered, e.g., in [9].

To introduce the effect studied and explained in this work, we first present the results of numerical modelling of Eq. (1) with initial conditions in the form $g_s(x)R_s(x)e^{ik_s x}$ for values of $k_s \in (k_0, 1]$, $\epsilon''(k_0) = 0$, ensuring that the effective mass, $1/\epsilon''_s$, is negative, see Fig. 1(a). Taking $k_s = 1$, i.e. fixing soliton parameters at the point corresponding to the zero of the group

velocity, we observe formation of the ideal solitary pulse [8]. The Fourier spectrum of this solution contains series of the equidistant peaks, the location of which is determined by the spectrum of the corresponding Bloch function $b(x, k_s = 1)$. Note, that the wave-numbers q , parameterizing the Fourier transform of ψ , $\psi = \int dx \tilde{\Psi}(q) e^{iqx}$, are linked with quasi-momenta k as $q = k \pm 2n$. Here and below $n = 0, 1, 2, \dots$ numbers the Brillouin zones. For values of $k_s \neq 1$ we have observed the quasi-solitonic pulses, which, while travelling, leave behind the trail of small amplitude radiation, Fig. 2(a). The radiation effect becomes noticeably stronger for $k_s \rightarrow k_0$. Spectra of the radiating solitons have a distinct peak, see Fig. 2(b), which is absent in the spectra of the ideal resting solitons. The overall results of the extensive series of numerical experiments unambiguously indicate that solitary pulses moving through the optical lattice continuously emit radiation with certain spectrally localized quasi-momenta. By analogy with electromagnetic case we term this radiation as *transition radiation of matter waves*.

The initial conditions used above in the form of the *sech* envelope superimposed on the Bloch function $g_s(x)e^{ik_s x}$ are difficult, though probably not impossible to prepare in the real experiments. However, current experimental techniques allow straightforward preparation of the gaussian matter-wave packets with spectrum centered around the zero quasi-momentum and setting lattices in motion. The lattice moving with velocity $2k_s$ will then effectively shift the central momentum of the wave packet to k_s . $2k_s$ equals to the group velocity of the free, i.e. without the lattice, matter waves with quasi-momentum k_s . In turn, the backward scattering of matter waves from the moving lattice is expected to create the second strong and other peaks in the spectrum of the wave-packet. The results of modelling of Eq. (1) with moving potential $\cos 2(x - 2k_s t)$ and initial conditions in the form of the gaussian packet are shown in Figs. 2(c,d). Taking into account shift of the axes, one can see that these results are in remarkable agreement with those obtained using the solitonic initial conditions, see Figs. 2(a,b). Good resolution of the radiation peaks in Figs. 2(b,d) suggests even that they can possibly be recorded experimentally.

To understand and give analytical interpretation of the observed radiation we develop a perturbative approach, allowing us to predict quasi-momenta and the amplitude of the emitted wave and, thereby allowing an estimate of the decay rate of a solitary pulse. To proceed we form the ansatz

$$\psi = \psi_s(x, \xi, t) + \varphi(t, x), \quad (5)$$

where the first term approximates the solitonic part of the wave function, $\psi_s = g_s(x)A_s(\xi, t)e^{ik_s x}$, and the second one is an arbitrary perturbation. Substituting (5)

into (1) and assuming that $|\varphi|$ is small we find that evolution of φ is governed by

$$i\partial_t\varphi + \hat{L}\varphi - 2|\psi_s|^2\varphi - \psi_s^2\varphi^* = S(x, t), \quad (6)$$

where $S(x, t) = -i\partial_t\psi_s - \hat{L}\psi_s + |\psi_s|^2\psi_s$ is the source term, which is different from zero because ψ_s is not an exact solution of Eq. (1).

The structure of the radiation tail observed in the numerical modelling corresponds to the spatially extended lattice eigenmode. The natural mechanism for excitation of a selected eigenmode from the continuum is the energy and wave-number resonance with one Fourier component of the source term S . The resonance condition ensures that there exists a lattice mode which is always in-phase and therefore interferes constructively with one Fourier component of the source term. The latter can be represented in the form $S = e^{ik_s x - i\epsilon_s t - i\kappa t} \sum_j h_j(x) f_j(\xi)$, where the sum is taken over all the terms appearing in the right-hand side after substitution of the explicit expression for the soliton and $h_j(x)$ are some functions with a period of π . Replacing $f_j(\xi)$ through their Fourier integrals $f_j(\xi) = \int dQ \tilde{f}_j(Q) e^{iQ\xi}$ and recalling that $\xi = x - \epsilon'_s t$, one can easily find that the lattice modes satisfying the resonance condition are those, which have quasi-momenta $k = k_r$ obeying the condition $\epsilon(k_r) = \kappa + \epsilon_s + \epsilon'_s Q_r$. $Q_r = Q(k_r)$ is the detuning of the wave-number of the resonant wave $q_r = k_r \pm 2n$ from the soliton quasi-momentum k_s , i.e. $Q_r = k_r \pm 2n - k_s$. Using that $\epsilon(k_r) = \epsilon(q_r)$ the resonance condition can be rewritten in the form

$$\epsilon(q_r) = \kappa + \epsilon_s + (q_r - k_s)\epsilon'_s. \quad (7)$$

The geometrical meaning of Eq. (7) is clear. The right-hand side of (7) equals to the energy of the Fourier component of the soliton (4), while its left hand side is simply the energy of the linear dispersive wave. Eq. (7) can be solved for q_r by plotting the tangent line to the periodically extended dispersion characteristic at the point $\epsilon = \epsilon_s$. Then one should make the parallel upshift of this tangent by κ and find points of the intersection with the dispersion characteristic itself. Topologically it is self-evident that only resting solitons do not produce any real roots of Eq. (7) and do not radiate into the lattice modes. For $\epsilon'_s \neq 0$ Eq. (7) has infinitely many real roots corresponding to different values of n . Root q_r for $n = 0$, i.e. when $q_r = k_r$, as a function of k_s is shown in Fig. 1(b). Dots on this graph show (k_r, k_s) pairs measured from the direct numerical modelling of Eq. (1). Modelling of Eq. (1) has not revealed any resonances in the Brillouin zones with $n \neq 0$. It indicates that coupling into the higher-order resonances is negligible, primarily because spectral strength of the source term is very weak for the values of Q_r with $n \neq 0$. Note, that the secondary less intense spectral peaks, seen in Figs. 2(b,d), are described by the peaks in the Fourier spectra of $b(x, k_{r,s})$,

and are given by $q_{r,s} = k_{r,s} \pm 2n$. At the same time, multiple roots of Eq. (7) are not linked by any simple algebraic expression.

In order to calculate the amplitude of the radiated wave we form the anzats

$$\psi \simeq \psi_s(x, \xi, t) + g_r(x) e^{ik_r x - i\epsilon_r t} W(t, \xi), \quad (8)$$

where subscript 'r' refers to the quantities calculated at $k = k_r$. Substituting (8) into Eq. (1) we take into account that $\hat{L}g_r(x) e^{ik_r x} W(t, \xi) \simeq -g_r(x) e^{ik_r x} \hat{E}_r W(\xi, t)$. The latter expression can be easily inferred by comparison with Eq. (3). Assuming that $\delta k_s \ll |k_s - k_r| \ll 2$, where δk_s is the width of the soliton in the quasi-momentum space and 2 is the width of the Brillouin zone, and disregarding terms nonlinear in W , one gets the averaged equation for the amplitude of the radiation field: $\vec{s} = i\partial_t \vec{W} + \hat{\mathcal{L}}_r \vec{W}$, where $\vec{s} = (P, -P^*)^T$, $\vec{W} = (W, W^*)^T$, $P = e^{i\xi(k_s - k_r)} [\alpha_4 \{\hat{E}_s - \hat{E}_{2s}\} R_s + \alpha_3 |R_s|^2 R_s]$, $\hat{D}_r[-i\partial_\xi] = -\epsilon_r + i\epsilon'_s \partial_\xi + \hat{E}_r[-i\partial_\xi]$,

$$\hat{\mathcal{L}}_r = \begin{bmatrix} -\hat{D}_r + \alpha_2 |R_s|^2 & \alpha_1 R_s^2 e^{2i\xi(k_s - k_r)} \\ -\alpha_1^* R_s^2 e^{2i\xi(k_r - k_s)} & \hat{D}_r^* - \alpha_2^* |R_s|^2 \end{bmatrix}, \quad (9)$$

$$\alpha_1 = \int dx g_s^2 g_r^{*2}, \alpha_2 = 2 \int dx g_s^2 |g_r|^2, \alpha_3 = \alpha_s \int dx g_s g_r^* - \int dx |g_s|^2 g_s g_r^*, \text{ and } \alpha_4 = \int dx g_s g_r^*.$$

The approximate solution we obtain for W is

$$W(t, \xi) \simeq -iC \{\Theta(\zeta\xi) - \Theta(\zeta\xi + \zeta t(\epsilon'_s - \epsilon'_r))\}. \quad (10)$$

Here $\zeta = \text{sgn}(\epsilon'_r - \epsilon'_s)$, Θ is the Heaviside function and C is the amplitude, which can not be generally expressed in a closed analytical form and, therefore, was calculated numerically. C characterizes the spectral intensity of the source term for $k = k_r$. Heaviside functions in Eq. (10) describe the tail of the radiation field having the length $t|\epsilon'_r - \epsilon'_s|$. The tail starts at the soliton ($\xi = 0$) and extends beyond ($\epsilon'_r < \epsilon'_s$) or in front ($\epsilon'_r > \epsilon'_s$) of it.

Substituting the ansatz (8) into the conservation law $\partial_t \int dx |\psi|^2 = 0$, we can estimate the rate, γ , of the transfer of particles from the soliton to the radiation: $\gamma = C^2 |\epsilon'_s - \epsilon'_r|$. Plot of $\log_{10} \gamma$ vs k_s for two values of κ is shown in Fig. 3(a). Naturally, the rate of transfer increases, when detuning $|k_r - k_s|$ decreases for $k_s \rightarrow k_0$, see Fig. 1(b). This is because for $k_s \rightarrow k_0$ the lattice mode is resonant with the most intense central part of the soliton spectrum. Contrary, $|k_r - k_s|$ increases for $k_s \rightarrow 1$, and the radiation amplitude decays almost exponentially. For example, semi-analytical Eq. (10) gives that the initial condition with $k_s = 0.87$ used to generate Fig. 2 has the initial decay rate 3×10^4 particles per second. Providing that this rate is constant in time, the soliton life-time would be $\simeq 0.033$ s. However, radiation carries away both density and momentum from the solitonic part of the field. Therefore solitonic parameters κ and k_s are in fact functions of time. In particular, we

have found that the radiation results in convergence of the soliton quasi-momentum to some limit value, which is always closer to 1 than the initial k_s . Thus, radiation emission slows the soliton. For example, taking initial conditions with $\kappa = 0.01$ and $k_s = 0.87$ we have observed that over 0.05s (1000 dimensionless time units) k_s shifts to $\simeq 0.887$, see Fig. 3(b), and κ to $\simeq 0.006$. The relatively small increase of k_s is accompanied by the decrease of the soliton decay rate, which drops, accordingly with plots shown in Fig. 3(a), from 3×10^4 to $\simeq 10^2$ particles per second. Let us stress again that the soliton life-time tends to infinity when $k_s \rightarrow 1$. Correspondingly, the estimated soliton life-time increases dramatically to $\simeq 10$ s. Fig. 3(b) also shows the numerically computed slowdown in the growth of the number of particles in the radiation component of the condensate. Soliton decay rate inferred from these data and corresponding theoretical points calculated for instant values of the soliton parameters κ and k_s are in good agreement, see inset in Fig. 3(b), which confirms validity of our theoretical method.

In summary, we have reported transition radiation by matter-wave solitons moving through the optical lattice. This effect extends family of the already known and related quantum radiative effects such as, e.g., sound emission by precessing quantized vortices [16] and by dark matter-wave solitons oscillating in a harmonic trap [17]. Note, also that our main conclusions and techniques can be used to predict and analyze radiation by spatial optical solitons moving in nonlinear photonic crystals [12]. This work was partially supported by the INTAS project 211-855.

- [1] S. Burger *et. al.*, Phys. Rev. Lett. **83**, 5198 (1999); J. Denschlag *et. al.*, Science **287**, 97 (2000).
- [2] K.E. Strecker *et. al.*, Nature (London) **417**, 150 (2002); L. Khaykovich *et. al.*, Science **296**, 1290 (2002).
- [3] B.P. Anderson and M.A. Kasevich, Science **282**, 1686 (1998); F.S. Cataliotti *et. al.*, Science **293**, 843 (2001); M. Greiner *et. al.*, Nature (London) **419**, 51 (2002); C. Fort *et. al.*, Phys. Rev. Lett. **90**, 140405 (2003).
- [4] S. Burger *et. al.*, Phys. Rev. Lett. **86**, 4447 (2001); O. Morsch *et. al.*, Phys. Rev. Lett. **87**, 140402 (2001); J.H. Denschlag *et. al.*, J. Phys. B **35**, 3095 (2002).
- [5] B. Eiermann *et. al.*, Phys. Rev. Lett. **91**, 060402 (2003).
- [6] Y.S. Kivshar and D.K. Campbell, Phys. Rev. E **48**, 3077 (1993).
- [7] O. Zobay *et. al.*, Phys. Rev. A **59**, 643 (1998); P. Meystre, *Atom Optics* (Springer, NY, 2001), Ch. 11.
- [8] K.M. Hilligse, M.K. Oberthaler, and K.P. Marzlin Phys. Rev. A **66**, 063605 (2002).
- [9] P.J.Y. Louis *et. al.*, Phys. Rev. A **67**, 013602 (2003).
- [10] R.G. Scott *et. al.*, Phys. Rev. Lett. **90**, 110404 (2003).
- [11] N.W. Ashcroft and N.D. Mermin, *Solid State Physics* (Saunders College, NY, 1976).

- [12] *Nonlinear Photonic Crystals*, R.E. Slusher and B.J. Eggleton, Eds., (Springer, 2003).
- [13] L.D. Landau, E.M. Lifshits, *Electrodynamics of Continuous Media* (Moscow, Nauka, 1992), Ch. 116.
- [14] Experimental control of the matter-wave dispersion using this technique has been recently demonstrated in Ref. [5].
- [15] V.V. Konotop and M. Salerno, Phys. Rev. A **65**, 021602 (2002).
- [16] L.M. Pismen, *Vortices in Nonlinear Fields* (Clarendon Press, Oxford, 1999), Ch. 4.
- [17] N.G. Parker *et. al.*, Phys. Rev. Lett. **90**, 220401 (2003).

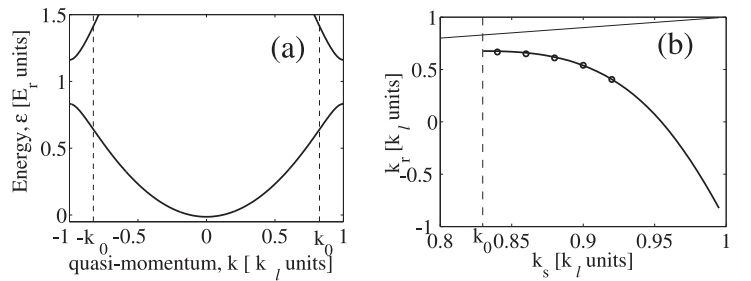


FIG. 1. (a) Energy-momentum diagram for the linear matter-waves in optical lattice: $n = 0$ Brillouin zone is shown. (b) Dependence of the radiation quasi-momentum, k_r , from the soliton quasi-momentum, k_s . Full diagonal line in (b) corresponds to $k_r = k_s$. Dots in (b) mark (k_s, k_r) pairs measured from the modelling of Eq. (1). Dashed vertical lines in (a) and (b) mark the $\pm k_0$ points with $\epsilon'' = 0$. $\beta = 0.33$

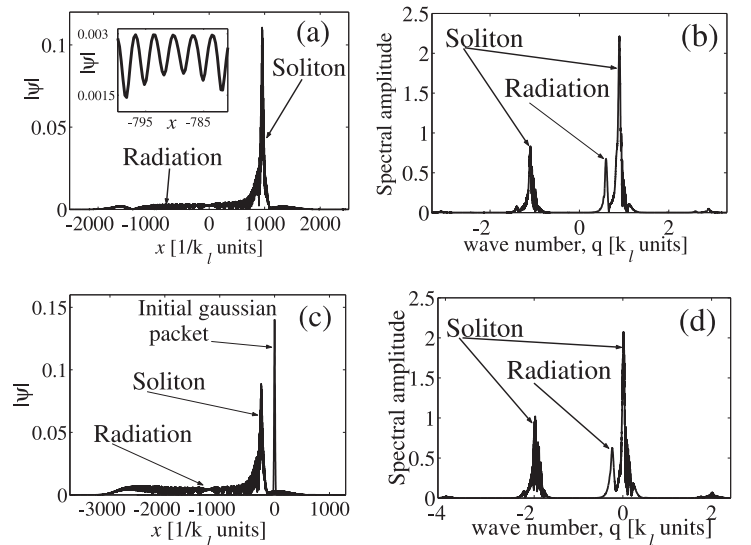


FIG. 2. Results of the direct numerical modelling of Eq. (1). (a,c) Square roots of the atomic density as functions of x . The inset in (a) shows fine details of the spatial profile of the radiation. (b,d) Corresponding Fourier spectra. (a,b) are obtained for the initial solitonic wave packet with $k_s = 0.87$ and $\kappa = 0.01$. (c,d) are obtained for the initial gaussian wave packets with the zero central momentum and lattice moving with velocity $2k_s = 1.74$. Integration time $t = 700$ corresponds to 0.035s. The physical number of particles in the soliton shown in Fig. 2(a) is $\simeq 10^3$, its velocity is $3 \times 10^{-3} m/s$ and width at the half-height is $\simeq 4 \mu m$.

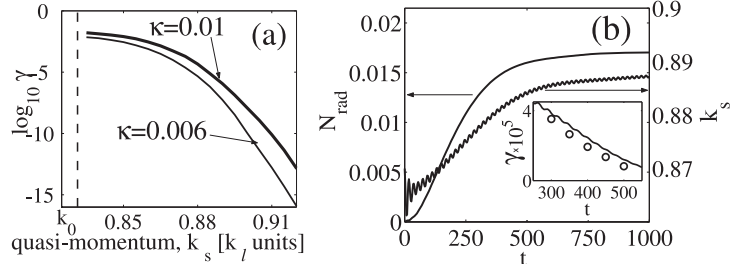


FIG. 3. (a) Logarithm of the particle transfer rate from the solitonic to the radiation part of the wave function as a function of the soliton quasi-momentum for $\kappa = 0.01$ and 0.006 . Dashed vertical line marks the $\epsilon'' = 0$ point. (b) Temporal evolution of the normalized number of particles N_{rad} in the radiation component of the field (left axis) and corresponding dynamics of the soliton quasi-momentum (right axis). N_{rad} is calculated as integral of $|\psi|^2$ over the tail behind the soliton. Estimate for physical number of particles in the radiation tail is given by $3 \times 10^3 N_{rad}$. Inset shows the soliton decay rate γ as function of t : solid line – numerical modelling and dots – theoretical results.